FATIGUE CRACK GROWTH IN WELDED RAILS

J.W. Ringsberg[*], B.L. Josefson and A. Skyttebol
Department of Applied Mechanics, Chalmers University of Technology, SE–412 96 Göteborg, Sweden
[*]E-mail: Jonas.Ringsberg@me.chalmers.se

ABSTRACT

The effect of welding residual and thermal stresses on fatigue crack growth in rail welds was studied. The residual stresses in a flash-butt weld were calculated by means of finite element (FE) analysis, and the results were in good agreement with experimentally determined residual stresses in a welded rail. The redistribution of the residual stresses in the welded rail was simulated using an FE model developed for train-track-rail interaction simulation. It was employed here for train traffic conditions at a straight track during heavy-haul operation conditions. The thermal stresses that occur in the rail due to variations in temperature between winter and summer were also accounted for in this FE model. The results from the stabilised stress response in the rail, after several wheel-rail contact load passages, were used to investigate the sensitivity in crack growth in the weld region using fracture mechanics. A number of parameters were varied, for example, the axle load, crack location, crack size and rail temperature.

1 INTRODUCTION

Railway rails are manufactured in sections of 25 - 120 m length which are joined in track by bolting or welding. Two advantages with welded rail sections in contrast to bolted ones are the lower maintenance cost and the improved dynamic behaviour of the train-track-rail system. There are primarily two rail welding processes which are used today, the flash-butt welding and alumino-thermic (thermite) welding processes. The residual stress-state in a thermite weld was measured by Webster et al. [1]; however, the flash-butt and thermite welding methods introduce a similar residual stress field in the foot, the web and the head of the rail. In addition, small inclusions or cracks can appear in a welded cross-section [2]. The thermite welding process generates cracks to a higher degree due to its casting nature, as compared with the flash-butt welding process. Defects in thermite welds are often lack-of-fusion, shrinkage cavities, hot tears, gas pockets and inclusions from entrapped slag or mould. Defects in flash-butt welds are almost always confined to iron oxide inclusions in the fusion zone, internal imperfections in the weld or microstructural alterations from post weld trimming of surfaces [3]. Mutton et al. [4] reported on surface cracks in the web of flash-butt welds and shrinkage cracks in thermite welds.

The train traffic situation at the Malmbanan (Iron-ore) line in the northern part of Sweden is studied. On this line, the train speed is low because of the high axle loads, typically 50 km/h. The axle load of a fully loaded freight car is 25 - 30 metric tonnes, and the annual load capacity on the line is 20 - 22 MGT. Cracks have been found in welded joints and the hypothesis was that the residual stress-state from the welding process, together with pre-existing cracks in the rail/weld, has great effect on the time to fatigue failure. A numerical simulation of the flash-butt welding process is carried out, and the residual stress-state is used as the initial conditions to a subsequent simulation of passing trains on a track using a train-track-rail interaction model. Thermal stresses in the rail due to variations in the ambient temperature are also incorporated. The results from the simulations are used in fatigue crack growth calculations of defects in the weld region using linear-elastic fracture mechanics; see Skyttebol et al. [5] for a thorough description of the numerical simulations and calculations.

2 FLOWCHART OF NUMERICAL SIMULATIONS AND ANALYSES

In this study on fatigue crack growth in a flash-butt welded rail, different sizes and locations of the cracks as well as different loading conditions are examined. The numerical simulations incorporate several steps and calculations, in order to make the fatigue assessment of the weld as realistic as possible, see Figure 1. The finite element (FE) method using the commercial FE code ABAQUS/Standard [6] is employed to simulate the welding process, the dynamic global train-track response and the local elasto-plastic stress response in the rail. The fatigue crack growth analyses are carried out in the commercial code SACC [7].
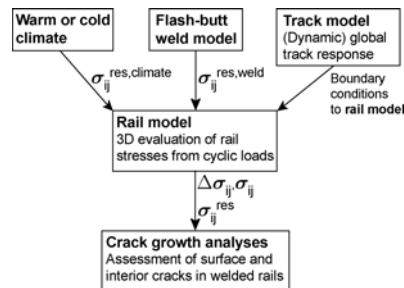
Figure 1: Flowchart of the fatigue evaluation of flash-butt welded rails.

3 MATERIAL CHARACTERISTICS

The rail material was the pearlitic UIC grade 900A (R260) rail steel. Its behaviour at room temperature was obtained from materials testing at 20°C and the behaviour at elevated temperatures was obtained from materials testing at 600°C. The tests showed, as could be expected, that both the yield stress and the Young's modulus drop to about half when the temperature is increased from 20°C to 600°C. For temperatures higher than 600°C, no tests were performed and thus, the behaviour at these temperatures was estimated [5].

The positions for susceptible crack growth were presumed to be well below the surface of the rail head, where elastic shakedown conditions prevail after repeated cyclic loading and redistribution of residual stresses, see Mutton et al. [4]. Consequently, a linear kinematic constitutive material model was used in the simulations, which in the welding analysis included also annealing behaviour of the material. The annealing behaviour of the material was accounted for following the annealing option in ABAQUS; the equivalent plastic strain and the backstress tensor are set to zero at the annealing temperature. The melting and annealing temperatures for the current material were 1470°C. In Figure 2, the characteristics of the UIC grade 900A material in a tensile test for different temperatures are defined by the dashed lines. The solid lines represent the elasto-plastic behaviour that was calculated using the linear kinematic hardening model. The temperature-dependent material data used in the thermo-mechanical analysis of the flash-butt welding process (see Section 4) are presented in Skyttebol et al. [5].
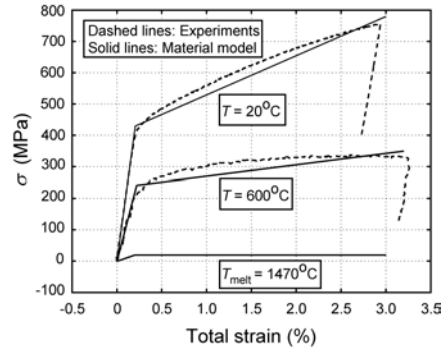
Figure 2: Material data from experiments and data used in the FE analysis with ABAQUS.

4 NUMERICAL SIMULATION OF FLASH-BUTT WELDING OF RAILS

Flash-butt welding is a resistance welding method. An electric potential is applied between two pieces of metal which are clamped adjacent to each other. This results in a current flow through the circuit which is sufficient to produce a flashing action. The metal is heated to the fusion point and the weld is completed by applying an upset force.

The welding operation comprises three steps: preheating, burning-off and upsetting. Preheating is performed by pressing the two rails together and separation of them as an electric current passes across the interface. In the second step, the edges are slightly parted and a low voltage is applied between the ends causing a flash arc. The surfaces are cleaned and uniformly heated during this step. In the third and last step, the upsetting, a force is applied rapidly, which forge the two ends together, and the molten metal between the ends are expelled.

The finite element simulation of the flash-butt welding process was carried out in a sequence, starting with an electro-thermal analysis that provides a temperature field history to the subsequent thermo-mechanical analysis; see Skyttebol et al. [5] for more details about the welding simulation. The option of geometrical nonlinearities in ABAQUS was used for the latter analysis, as well as for the train-track-rail interaction analysis with the rail model in Section 5.

5 NUMERICAL SIMULATION OF TRAIN-TRACK-RAIL INTERACTION

An FE tool was developed in previous work for the analysis of rolling contact fatigue (RCF) of railway rails; see Ringsberg et al. [8] for details. It can mimic the wheel-rail rolling-sliding contact on a track, since it incorporates both the dynamic global track response and the three-dimensional local elasto-plastic contact conditions in the rail head. Two FE models, for track and rail, which are coupled by time-dependent boundary conditions, form the FE tool. An elastic FE analysis using the track model calculates time-dependent displacements at two cross-sections 12 cm apart; these are then used as boundary conditions in an elasto-plastic FE analysis using the rail model. As a result, the influences of both the dynamic global track response and the three-dimensional local elasto-plastic material response in the rail are incorporated in the rail fatigue or stress analysis.

5.1 Contact loads

The Malmbanan line between Kiruna (Sweden) and Narvik (Norway) is two-way-trafficked on one track, i.e. loaded freight cars run from Kiruna to Narvik where the ore is unloaded before the cars return (unloaded) to Kiruna on the same track. The loaded iron-ore cars have an average axle load of 30 metric tonnes and they run at 50 km/h on straight track. Because the loaded iron-ore cars contribute the most to RCF damage of the rail, their contact loads were used here.

Train traffic on a straight track was simulated, and therefore, the wheel-rail contact position was at the symmetry line in the rail longitudinal direction. The wheel-rail contact loads acting on the rail model, in the normal, longitudinal, and lateral directions, were represented by moving distributed normal pressure and shear stress distributions [8]. The distributions were calculated according to the Hertz theory of rolling contact between two elastic non-conforming solids with smooth and continuous contact surfaces.

The 30 metric tonne axle load corresponded to a rail normal force of 147×10^3 N (peak normal pressure 1401 MPa). The magnitude of the tangential loads was estimated from field measurements at track (using resultant contact forces in the normal, longitudinal and lateral rail directions) and from material testing by twin-disc tests. The in-plane rail longitudinal force component due to traction was modelled using the traction coefficient 0.35. It was a representative value obtained from field measurements, and also from twin-disc tests (dry contact) for the current wheel and rail materials [8]. As straight track was modelled, only a small contribution from the in-plane rail lateral force component was in action using the traction coefficient 0.10. Hence, there was a shear stress distribution for fully slipping contact both in the longitudinal and lateral directions of the rail. In addition, the train-track interaction calculations were carried out using realistic traffic data for (static) 30 metric tonnes axle load and train speed 50 km/h. However, to include possible dynamic effects on the contact loads, calculations were made for three axle loads for comparison: 30, 35 and 40 metric tonnes.

5.2 Thermal stresses and application of the FE tool

Railway rails in Sweden are normally laid at the reference temperature 20°C where the rail is (assumed) stress-free when it is clamped to the sleepers. However, the ambient temperature near the Malmbanan line varies annually between -40°C and 40°C, which gives rise to thermal stresses in the rail. For this reason, the temperature effect on the residual stress-state was also investigated for the case of the 30 metric tonnes axle load. All together, four initial stress-state conditions of a rail were analysed with the FE tool: (a) residual stress-free rail, (b) residual stress field from the flash-butt welding process, $T_{ref} = 20$°C, (c) residual stress field from the flash-butt welding process and superposed stresses from cold climate during the winter, $T_{cold} = -40$°C, and (d) residual stress field from the flash-butt welding process and superposed stresses from a warm climate during the summer, $T_{hot} = 40$°C.

A user-supplied subroutine was formulated in the FE code ABAQUS in order to transfer the results from the flash-butt welding FE simulation to the rail FE model calculations. It was done by interpolation, between nodes, of node average stresses. These stresses became the initial conditions to the first step of the rail FE model calculation. No contact loads were applied for this step, and equilibrium was reached after some iterations. The thermal stresses due to colder or warmer climate were added as $E \cdot \alpha \cdot \Delta T$ using the subroutine, i.e. in the longitudinal direction of the rail, where ΔT is the deviation in temperature from the reference temperature, E is the Young's modulus and α is the thermal expansion coefficient; see reference [5] for details.

6 FATIGUE CRACK GROWTH CALCULATIONS IN 2D

The results from the flash-butt welding FE simulation were verified against residual stress measurements and there was good agreement [5]. For the longitudinal stress field there were compressive stresses in the rail head and rail foot, and tensile residual stresses in the web. The train-track-rail interaction calculations showed large stress ranges due to global bending of the rail in the lower part of the rail head, whereas the stress ranges calculated in the web and rail foot were much lower. Apart from the contact zone at the rail head, the weld material experienced elastic shakedown after very few load passages. For this reason, linear-elastic fracture mechanics was applicable to study growth of defects in the weld region using the code SACC. Because the shear stress ranges in the region of interest in the rail head were considerable less than the normal stress ranges, the stress-intensity factor was calculated using the normal stress component in the uncracked material normal to the plane with the defect.

Three different defects were considered: (1) an embedded circular crack at mid level of the rail head subject to vertical stress ranges, (2) an embedded circular crack in the rail head just above the web also subject to vertical stress ranges, and (3) a half-circular surface crack (crack length/mouth on the surface divided by crack depth = 2) at the lower part of the rail head subject to longitudinal stress ranges. The first two cases correspond to inclusion defects or lack-of-fusion defects, while the third case corresponds to a crack starting from a defect caused by the final trimming of the web and rail head. For all cases, two standard cases in SACC were used: an embedded crack (with zero eccentricity) in a plate with finite thickness, and a circular surface crack in a plate with finite thickness. The representative plate thickness was $t = 40$ mm, and the size of the crack area, A_{crack}, was varied between 5 and 100 mm^2.

A Paris type crack growth law was used with $C = 2.47 \cdot 10^{-9}$ (growth rate in mm/cycle and stress in MPa) and the exponent $n = 3.33$. The stress ratio, $R = \sigma_{min} / \sigma_{max}$, was high, $R = 0.7 - 0.9$, which means that existing cracks are fully open during the load passage. The threshold stress-intensity factor was assumed $\Delta K_{th} = 2$ MPa$\sqrt{m}$ and the fracture toughness was $K_{IC} = 40$ MPa$\sqrt{m}$. The SACC calculations were stopped when the maximum stress-intensity factor reached the fracture toughness. Figure 3 shows the results for the different axle loads (left), and for the examples (b) - (d) which had residual stresses as initial conditions and axle load 30 metric tonnes (right), see Section 5.2. The example (a) that was initially free from residual stresses showed no crack growth of the defects. One traffic year is 870 500 wheel passages, and "infinite life/no crack growth", i.e. $K < K_{th}$, is defined here as 50 traffic years.
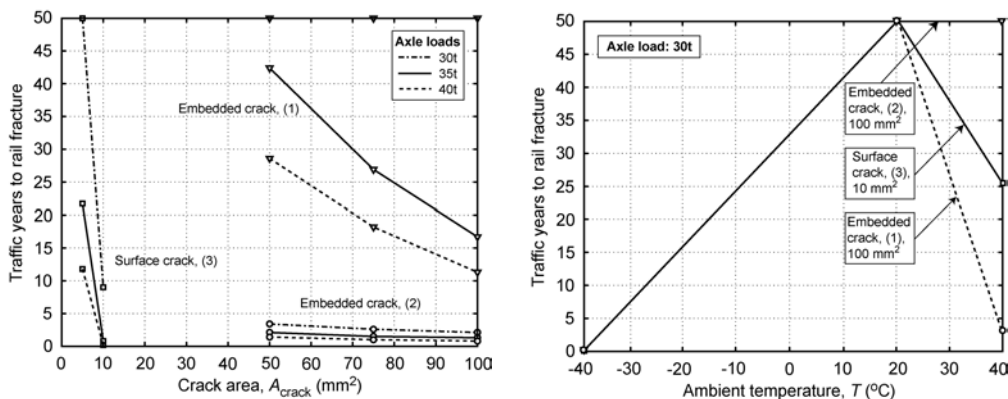
Figure 3: Left: traffic years vs. crack area; Right: traffic years vs. ambient temperature.

The sizes of the surface cracks were less than the sizes of the embedded cracks. Despite this, the surface cracks in the weld were more dangerous than the embedded cracks in the web-rail head area. The time to fatigue failure was strongly dependent on the ambient temperature, where the lowest temperature was the most damaging with respect to crack growth. Finally, the size and direction of the crack is of importance, in particular transverse cracks seem to be the most likely to occur in the area where the web meets the rail head.

7 ONGOING WORK: FATIGUE CRACK GROWTH CALCULATIONS IN 3D

The fatigue crack growth calculations presented in the previous section were performed using standard cases for two-dimensional crack growth. In ongoing work, the fatigue crack growth evaluation is carried out using the commercial code BEASY [9] instead of SACC. With this code, it is possible to make advanced three-dimensional crack growth analyses. The embedded inclusion defects in the rail head, for example, are represented by spherical defects in the BEASY rail model. The influence of residual stresses on crack growth from the flash-butt welding and train traffic operation simulations, as well as from variation in temperature, is of course accounted for following the calculation procedure in Figure 1. The results from the BEASY calculations will, except for the fatigue life, give also the path of crack advance in the rail.

8 REFERENCES

[1]   Webster PJ, Mills G, Wang XD, Kang WP and Holden TM. Residual stresses in alumino-thermic welded rails. *Journal of Strain Analysis*, **32**, 389–400, 1997.

[2]   Cheesewright PR. The improvement of thermit weld reliability. In *Proceedings of the seminar "Rail Technology"* in Nottingham, UK, September 21–26, 1981 (Organized by the British Rail Research and Development Division and the Association of American Railroads), pp. 305–320, 1981.

[3]   Feddersen CE and Broek D. Fatigue crack propagation in rail steels. In: Rail steels – Developments, processing and use. *ASTM STP 644*, Stone DH, Knupp GG, editors. pp. 414–429, 1976.

[4]   Mutton PJ, Epp KJ, Alvarez E and Lynch M. A review of wheel-rail interaction and component performance under high axle load conditions. In *Proceedings of the Sixth International Conference on Contact Mechanics and Wear of Rail/Wheel Systems (CM2003)* in Göteborg, Sweden, June 10–13, 2003 (Editors A. Ekberg, E. Kabo and JW Ringsberg), Vasastadens Bokbinderi AB, Göteborg, Sweden, pp. 273–278, 2003.

[5]   Skyttebol A, Josefson BL and Ringsberg JW. Fatigue crack growth in a welded rail under the influence of residual stresses. Research Report 2003:6, Department of Applied Mechanics, Chalmers University of Technology, Göteborg, Sweden, 2003. (Accepted for publication in *Engineering Fracture Mechanics*.)

[6]   Hibbitt, Karlsson & Sorensen. ABAQUS/Analysis User's Manual version 6.4. ABAQUS, Inc., Pawtucket, RI, USA, 2003.

[7]   SACC Version 4.1, revision 9, Det norske Veritas, Stockholm, Sweden, 2003.

[8]   Ringsberg JW, Bjarnehed H, Johansson A and Josefson BL. Rolling contact fatigue of railway rails – finite element modelling of residual stresses, strains and crack initiation. *Proc IMechE, Part F, Journal of Rail and Rapid Transit*, **214**, 7–19, 2000.

[9]   Computational Mechanics BEASY. BEASY version 9.0 release 1. Ashurst Lodge, Ashurst, Southampton, UK, 2004. (Website: www.beasy.com)